Heliyon 10 (2024) e23828

Contents lists available at ScienceDirect

Heliyon

journal homepage: www.cell.com/heliyon

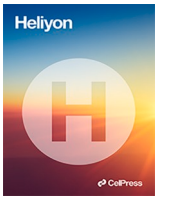

# Overexpression of SLC35F2 is a potential prognostic biomarker for lung adenocarcinoma

Qingzhu Zheng [a,1], Mingjie Li [a,1], Yingkun Qiu [a], Jiahao Yang [b], Yingping Cao [a,*]

[a] Department of Clinical Laboratory, Fujian Medical University Union Hospital, Fuzhou, 350001, China
[b] Department of Laboratory Medicine, School of Medical Technology and Engineering, Fujian Medical University, Fuzhou, 350004, China

ARTICLE INFO

*Keywords:*
LUAD
SLC35F2
The cancer genome Atlas
Biomarker
Prognosis

ABSTRACT

*Objective:* To explore the potential clinical and prognostic significance of Homo sapiens solute carrier family 35 member F2 (SLC35F2) in the context of lung adenocarcinoma (LUAD).
*Methods:* The expression pattern of SLC35F2 in LUAD tissues and normal tissues was analyzed in The Cancer Genome Atlas (TCGA) datasets and validated in 12 pairs of fresh clinical LUAD tissues and their corresponding adjacent normal tissues using quantitative real-time PCR (qRT-PCR) and western blotting. Immunohistochemistry (IHC) was used to assess the protein expression of SLC35F2 in 60 paraffin-embedded LUAD tissues, and its associations with clinicopathological parameters were further examined. The prognostic significance of SLC35F2 mRNA expression was also evaluated using the Kaplan-Meier method, and Cox regression models in LUAD patients from the TCGA database. The potential utility of SLC35F2 as an indicator of recurrence or metastasis was explored through the follow-up of selected clinical LUAD cases. Lastly, gene set enrichment analysis (GSEA) was conducted to investigate the underlying biological mechanisms and signaling pathways.
*Results:* Bioinformatics analysis utilizing the TCGA database indicated that SLC35F2 mRNA exhibited heightened expression in LUAD tissues when compared to normal tissues. These findings were further substantiated through the examination of 12 pairs of clinical LUAD tissues and their corresponding adjacent normal tissues, employing qRT-PCR and western blotting techniques. IHC results from a cohort of 60 LUAD patients demonstrated an up-regulation of SLC35F2 in 38 out of 60 individuals (63.3 %), which exhibited a significant correlation with tumor size, lymph node metastasis, and clinical stage (all $P < 0.05$). Both the Kaplan-Meier curve and the Cox proportional hazard analyses indicated a strong association between the up-regulation of SLC35F2 mRNA expression and unfavorable overall survival (OS) in patients with LUAD, as observed in the TCGA datasets ($P < 0.05$). The follow-up findings from select clinical LUAD cases provided evidence that the expression of SLC35F2 could serve as a dependable biomarker for monitoring the recurrence or metastasis. Additionally, the GSEA highlighted the enrichment of apoptosis, adhesion, small cell lung cancer (SCLC), and p53 signaling pathways in the subgroup of LUAD patients with elevated SLC35F2 expression.
*Conclusion:* SLC35F2 exhibited an up-regulated in both mRNA and protein expression, rendering it a valuable independent prognostic indicator for patients diagnosed with LUAD.

* Corresponding author. Department of Clinical Laboratory, Fujian Medical University Union Hospital, 29# Xinquan Rd, Fuzhou, 350001, Fujian, China.
*E-mail address:* caoyingping@aliyun.com (Y. Cao).
[1] Qingzhu Zheng and Mingjie Li contributed equally to this study.

https://doi.org/10.1016/j.heliyon.2023.e23828
Received 29 March 2023; Received in revised form 5 December 2023; Accepted 13 December 2023
Available online 16 December 2023

## 1. Introduction

Lung cancer (LC) is widely recognized as a significant contributor to global cancer-related mortality, ranking second in terms of incidence and highest in terms of fatality [1]. Non-small cell lung cancer (NSCLC) accounts for approximately 85 % of all lung cancer cases and can be categorized into three histological subtypes: lung adenocarcinoma (LUAD), lung squamous cell carcinoma (LUSC), and large cell carcinoma [2,3]. Among these subtypes, LUAD stands out as the most prevalent subtype of NSCLC [4].

Personalized treatment strategies for individuals with LUAD, comprising of surgical interventions, chemoradiotherapy, and molecular-targeted therapy, are implemented based on factors such as tumor dimensions, classifications, clinical staging, and histological grades [5]. As specific clinical symptoms of LUAD are absent in the early stage, most patients receive a diagnosis during advanced stages, resulting in exceedingly unfavorable clinical outcomes. Presently, the diagnosis of LUAD patients commonly involves imaging techniques and serological tests. Nevertheless, limitations in methodology, such as relatively diminished sensitivity and specificity, alongside concerns regarding high-dose radiotherapy and other factors, pose challenges to the early screening of LUAD patients [6–9]. Despite some advancements in diagnosis and treatment in recent times, the underlying mechanisms of LUAD remain inadequately explored. Consequently, exploring innovative biomarkers that align with treatment strategies and prognosis assessment holds the potential to enhance the overall survival (OS) rate and clinical outcomes of LUAD patients.

Homo sapiens solute carrier family 35 member F2 (SLC35F2) (Genebank No. NM 017515) also known as homo sapiens novel protein 1 (HSNOV1), was initially identified in ataxia telangiectasia syndrome by Stankovic et al. [10] in 1997. It belongs to the membrane binding carrier superfamily and is involved in the transport of various substances, including ions, drugs, metabolites, and vitamins [11]. Additionally, SLC35F2 is closely related to members of the Ras oncogene family (RAB39) and is located on the long arm of human chromosome 11. This gene not only plays a role in the formation of the blood-brain barrier but is also highly expressed in adult salivary glands [12,13]. Furthermore, SLC35F2 shares a high degree of similarity with the lung squamous cell cancer-related gene (LSCC3), which is associated with the progression of LUSC. Its expression level is higher in cancerous tissues compared to normal tissues [14]. Several studies focused on examining the expression and biological functions of SLC35F2 in various malignancies. For instance, Nyquist et al. [15] demonstrated that SLC35F2 expression is significantly correlated with androgen levels in prostate cancer and is regulated by the androgen receptor signaling axis. Kotolloshi et al. [16] showed that SLC35F2, a sporadically mutated transporter in the untranslated region, plays a crucial role in promoting the growth, migration, and invasion of bladder cancer (BC) cells. He et al.'s research results indicated that SLC35F2 contributes to the carcinogenesis of papillary thyroid carcinoma (PTC) through the mitogen-activated protein kinase and other pathways [17]. Moreover, SLC35F2 has been identified as a key factor in the biological function of YM155, a well-known anticancer compound. Conversely, SLC35F2 has also been used as a clinical biomarker to assess the effectiveness of YM155 chemotherapy [18]. Therefore, SLC35F2 could be a suitable biomarker for evaluating treatment strategies and prognosis in malignant tumors. Chandrasekaran et al. [19] demonstrated that ubiquitin-specific protease 32 (USP32) confers resistance to YM155 in cancer cells by destabilizing the protein level of SLC35F2. This finding suggests a novel approach to treat tumors that are resistant to small-molecule drugs. Bu et al. [20] revealed a significant correlation between the overexpression of SLC35F2 and pathological staging in NSCLC. However, the precise function, mechanism, and prognostic value of SLC35F2 expression in LUAD have yet to be elucidated.

The current investigation aimed to assess the expression pattern and prognostic significance of SLC35F2 in LUAD, with the objective of determining its potential as a valuable biomarker for the clinicopathological characteristics and prognosis of LUAD patients.

## 2. Materials and methods

### 2.1. Data mining

The transcriptome data and corresponding clinical information of patients with LUAD tissues and normal tissues were obtained from The Cancer Genome Atlas (TCGA) database (https://cancergenome.nih.gov/). The LUAD datasets consisted of 497 cancer tissues and 54 normal tissues. Subjects with insufficient clinical information were excluded. The results were analyzed using R software with edgeR, limma, and beeswarm package. TCGA database is a freely accessible platform.

### 2.2. Patients and specimens

A total of 12 pairs of fresh LUAD tissues and their corresponding adjacent normal tissues were collected from the Department of Thoracic Surgery of Fujian Medical University Union Hospital. The participants included 5 men and 7 women, with a median age (interquartile range, IQR) of 57 years (55–65). The clinical pathological stage consisted of 9 cases in stages I and II, and 3 cases in stages III and IV. All fresh tissues were rapidly frozen in liquid nitrogen and stored at −80 °C. Additionally, 60 pairs of paraffin-embedded LUAD tissues and their corresponding adjacent normal tissues were obtained from surgically resected specimens diagnosed as LUAD at Fujian Medical University Union Hospital between January 2020 to January 2021. The clinical characteristics are presented in Table 1. None of the patients received neoadjuvant chemotherapy or any other treatment before tissue sampling. Pathological diagnoses and clinicopathological staging were determined according to the classification of the World Health Organization (WHO) and the American Joint Committee on Cancer (AJCC). To assess whether SLC35F2 expression could serve as an indicator of LUAD recurrence or metastasis, we randomly selected 20 LUAD cases from the aforementioned 60 patients for follow-up. The inclusion criteria included

patients with complete personal information, regular follow-up visits and treatment, and comprehensive auxiliary examination data. The expression of SLC35F2 was evaluated through immunohistochemical staining (IHC) scoring. The follow-up period ranged from 9 to 30 months, with a median follow-up time of 20 months. Follow-up information, including the date of surgery, treatment methods, and recurrence status was collected. The occurrence of recurrence or metastasis was assessed by professional medical institutions and physicians. Informed consent was obtained from all patients, and the study was approved by the Institutional Review Board of Fujian Medical University Union Hospital (Ethics No.: 2021KY050).

### 2.3. RNA extraction, reverse transcription, and quantitative real-time PCR (qRT-PCR)

Total RNA was isolated from 12 pairs of fresh frozen LUAD tissues and their corresponding adjacent normal tissues using the TRIzol reagent (Invitrogen, NY, USA) following the manufacturer's instructions. Subsequently, 2 μg of total RNA was reverse transcribed into single-stranded cDNA using a reverse transcription Kit (Promega, USA). The reverse transcription reaction system had a total volume of 20 μl, comprising Nuclease-Free Water (0.6 μl), GoScriptTM 5X Reaction Buffer (4 μl), MgCl2 (25 mM, 4 μl), Oligo(dT)15 Primer (500 μg/ml, 0.5 μl), Random Primers (500 μg/ml, 0.5 μl), PCR Nucleotide Mix (1 μl), Recombinant RNasin Ribonuclease Inhibitor (0.4 μl), GoScriptTM Reverse Transcriptase (1 μl), RNA (2 μg), and supplemented with Nuclease-Free Water to reach the total volume. The conditions for the reverse transcription reaction included extension at 42 °C for 15 min, followed by reverse transcriptase inactivation at 70 °C for 15 min qRT-PCR analysis was conducted using the BRYT Green dye detection system (Promega, USA), with Glyceraldehyde-3-phosphate dehydrogenase (GAPDH) serving as an endogenous control. The qRT-PCR system had a total volume of 20 μl, consisting of Nuclease-Free Water (7 μl), Forward Primer (10 μM, 0.4 μl), Reverse Primer (10 μM, 0.4 μl), GoTaq qPCR Master Mix, 2X (10 μl), CXR 100X (0.2 μl), cDNA (2 μl). The conditions for qRT-PCR include pre-denaturation (95 °C, 2 min, 1 cycle), thermal cycle (95 °C, 15 s and 60 °C, 1 min, 40 cycles), and dissociation stage. The relative mRNA expression level of SLC35F2 was determined using the 2-ΔΔCT method. The primer sequences used were as follows: SLC35F2: 5′-TGGGACTGGAAAATTGCC.

CT-3' (forward) and 5′-TAGAGGTCCGCTGTCAGGAT-3' (reverse); and GAPDH: 5′-GGTGTGAACCATGAGAAGTATGA-3' (forward) and 5′-GAGTCCTTCCACG.

ATACCAAAG-3' (reverse). All tests were performed in triplicate.

### 2.4. Western blotting

Total proteins were extracted from 12 pairs of fresh frozen LUAD tissues and their corresponding adjacent tissues using the Whole Protein Extraction Kit (Solarbio, China). The Omni-EasyTM Instant BCA Protein Assay Kit (EpiZyme, China) was employed to

**Table 1**
Relationships between SLC35F2 expression and clinicopathological parameters in clinical LUAD patients.

| Variables | N(%) | SLC35F2 expression | | *P* value |
|---|---|---|---|---|
| | | Low (%) | High (%) | |
| Total | 60 | 22 (36.7 %) | 38 (63.3 %) | |
| Age (years) | | | | 0.306 |
| <60 | 33 | 14 (63.6 %) | 19 (50.0 %) | |
| ≥60 | 27 | 8 (36.4 %) | 19 (50.0 %) | |
| Gender | | | | 0.205 |
| Male | 29 | 13 (59.1 %) | 16 (42.1 %) | |
| Female | 31 | 9 (40.9 %) | 22 (57.9 %) | |
| Tumor size | | | | **0.011** |
| <3 cm | 46 | 21 (95.5 %) | 25 (65.8 %) | |
| ≥3 cm | 14 | 1 (4.5 %) | 13 (34.2 %) | |
| Depth of invasion | | | | 0.292 |
| T1-T2 | 57 | 22 (100 %) | 35 (92.1 %) | |
| T3-T4 | 3 | 0 (0 %) | 3 (7.9 %) | |
| Lymph node metastasis | | | | **0.002** |
| N0 | 43 | 21 (95.5 %) | 22 (57.9 %) | |
| N1–N3 | 17 | 1 (4.5 %) | 16 (42.1 %) | |
| Distant metastasis | | | | 0.148 |
| M0 | 55 | 22 (100 %) | 33 (86.8 %) | |
| M1 | 5 | 0 (0 %) | 5 (13.2 %) | |
| Clinical stage | | | | **0.011** |
| I & II | 46 | 21 (95.5 %) | 25 (65.8 %) | |
| III & IV | 14 | 1 (4.5 %) | 13 (34.2 %) | |
| CEA, ng/mL | | | | 0.106 |
| <5 | 47 | 20 (90.9 %) | 27 (71.1 %) | |
| ≥5 | 13 | 2 (9.1 %) | 11 (28.9 %) | |
| Cyfra21–1, ng/mL | | | | |
| <3.3 | 37 | 15 (68.2 %) | 22 (57.9 %) | 0.583 |
| ≥3.3 | 23 | 7 (31.8 %) | 16 (42.1 %) | |

Abbreviations: SLC35F2, Homo sapiens solute carrier family 35 member F2; CEA, Carcinoembryonic antigen; Cyfra21-1, Cytokeratin 19 fragment.

determine the protein concentration. Equal quantities (25 μg) of protein samples in each well were separated on a 10 % sodium dodecyl sulfate-polyacrylamide gel electrophoresis (SDS-PAGE) and transferred to polyvinylidene fluoride membranes (PVDF) (Millipore, USA). The PVDF membranes were blocked with 5 % fat-free milk in Tris-buffered saline (TBS)/0.1 % Tween 20 at room temperature for 1 h, followed by overnight incubation at 4 °C with primary antibodies against SLC35F2 (1:400, PA5-42470, Invitrogen, USA) and GAPDH (1:5000, ET1601-4, HUABIO, China). On the following day, the membranes were washed and incubated with horseradish peroxidase-conjugated secondary antibody (1:50000, HA1001, HUABIO, China) for 1 h at room temperature. The immunoreactive bands were visualized using ECL Western blotting substrate (Pierce, Thermo Scientific, USA) and detected on a chemiluminescence imager (Bio-Rad ChemiDoc MP, USA).

### 2.5. Immunohistochemical staining (IHC)

LUAD tissues and their corresponding adjacent normal tissues from 60 patients were fixed using formalin and embedded in paraffin. Subsequently, 5-μm-thick paraffin sections were prepared and underwent deparaffinization and rehydration. IHC studies were conducted using a commercially available kit (Fuzhou Maixin Biotech, China), following the manufacturer's instructions and utilizing the Rabbit anti-human SLC35F2 antibody (1:200, PA5-42470, Invitrogen, USA). Special sections of LUAD tissue sections with consistently positive SLC35F2 protein served as a positive control, while phosphate buffer saline (PBS) was used as a negative control in place of the primary antibody. The IHC staining results were evaluated and scored by two pathologists independently and in a blinded manner. The degree of IHC staining was assessed based on the score of positive cells and staining intensity. The score for positive cells was as follows: 0: 0–5 %; 1: 6–25 %; 2: 26–50 %; 3: 51–75 %; 4: >75 %. The score for staining intensity was as follows: 0: no staining; 1: weak staining, light yellow; 2: moderate staining, yellowish brown; 3: strong staining, brown. An overall score was calculated by multiplying the positive cells score and the staining intensity score. A final staining score of ≤3 indicated low SLC35F2 expression, while a score of 4–12 indicated high SLC35F2 expression.

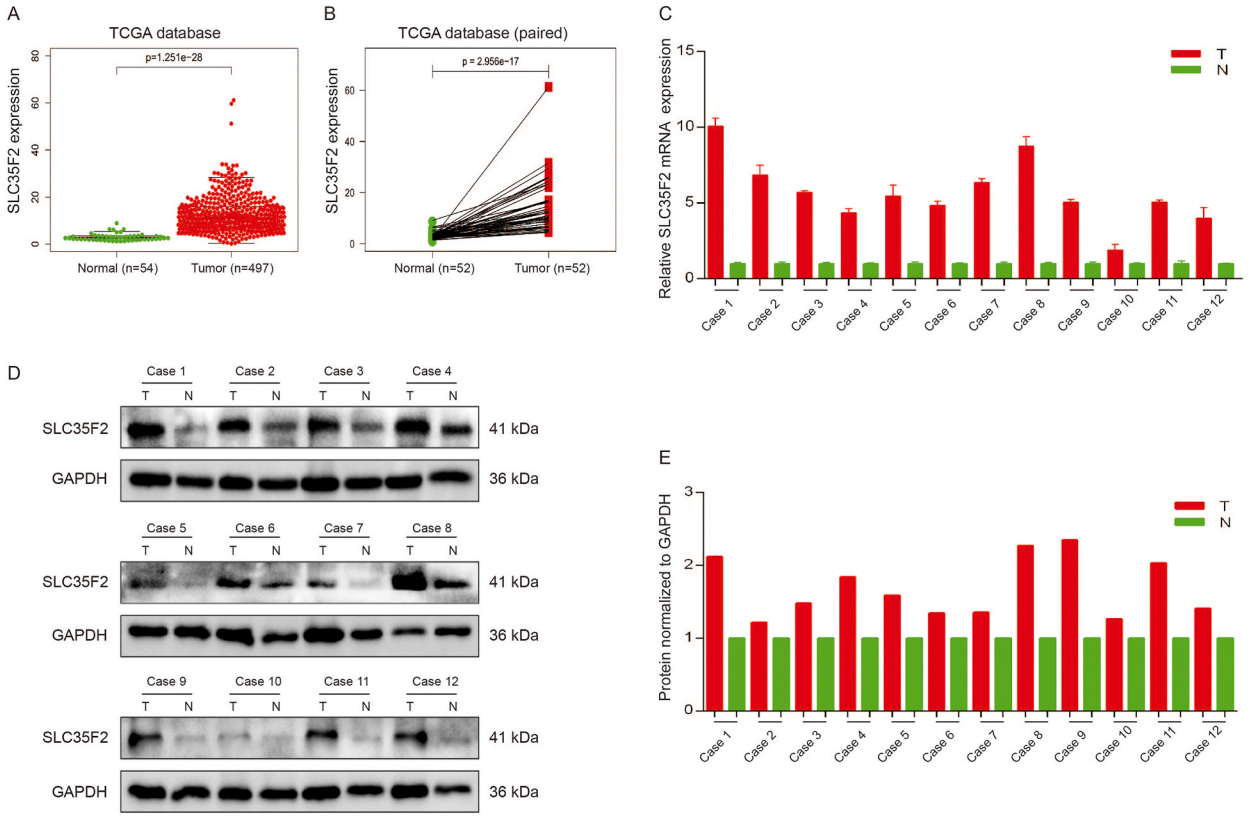


**Fig. 1.** Expression analysis of SLC35F2 in LUAD. (A) SLC35F2 mRNA exhibits up-regulated in LUAD tissues compared with normal tissues in TCGA datasets (tumor, n = 497, normal, n = 54, $P < 0.001$). (B) The differential expression analysis of paired tissue samples in TCGA datasets (paired *t*-test, tumor, n = 52, normal, n = 52, $P < 0.001$). (C, D) Both mRNA and protein expression of SLC35F2 in 12 pairs of fresh LUAD tissues and corresponding adjacent normal tissues were assessed using qRT-PCR (C) and western blotting (D). (E) The quantification and normalization of SLC35F2 protein levels were conducted using GAPDH. T denotes LUAD tumor tissues, while N represents matched adjacent normal tissues.

### 2.6. Chemiluminescence immunoassay (CLIA) for conventional tumor markers

The serum concentrations of carcinoembryonic antigen (CEA) and cytokeratin 19 fragment (CYFRA21-1) were assessed utilizing the CLIA kit of Cobas6000 analyzer (Roche, Mannheim, German), following the manufacturer's instruction. The cut-off values of CEA and CYFRA21-1 were established as follows: CEA, 5.0 ng/ml; CYFRA21-1, 3.3 ng/ml.

### 2.7. Gene set enrichment analysis (GSEA)

To explore the underlying molecular mechanism of SLC35F2 in the tumorigenesis and progression of LUAD. GSEA was used to determine whether a predefined set of genes exhibited a notable statistical distinction between the groups with high and low SLC35F2 expression, as obtained from the TCGA database [21,22]. Gene sets that displayed a normalized enrichment score (NES) $> 1.0$, a nominal (NOM) $P$-value $<0.05$, and a false discovery rate (FDR) q-value $<0.25$ were regarded as significantly enriched.

### 2.8. Statistical analysis

Statistical analysis and graphic visualization were conducted using the R software package (v.3.6.1), SPSS Statistics (v.22.0), and GraphPad Prism (v.6.02). The disparities in SLC35F2 mRNA expression levels between cancerous and normal tissues were evaluated through unpaired and paired Student's t-tests. The association between SLC35F2 expression and clinical characteristics of LUAD was examined using the Chi-square test or Fisher exact test. The OS of LUAD patients in the TCGA datasets was estimated using the Kaplan-Meier method and assessed via the log-rank test. Univariable and multivariable Cox regression models were employed to assess the impact of clinical characteristics and SLC35F2 expression levels on the prognosis of LUAD patients, as obtained from the TCGA datasets. The Cox regression model enabled the calculation of hazard ratio (HR), 95 % confidence interval (CI), and $P$ value, with the R software and survival package utilized for statistical analysis and model establishment. $P$ value $< 0.05$ was considered statistically significant.

## 3. Results

### 3.1. SLC35F2 exhibited elevated expression in LUAD tissues compared to normal tissues

Gene expression data analysis from the TCGA database demonstrated a noteworthy upregulation of SLC35F2 mRNA levels in 497 LUAD tissues compared to 54 normal tissues (unpaired 2-sample $t$-test, $P < 0.001$). This finding was consistent with the results obtained from 52 pairs of LUAD tissues and their matched adjacent normal tissues (paired $t$-test, $P < 0.001$) (Fig. 1 A, B). The elevation of SLC35F2 mRNA in LUAD tissues was further confirmed through qRT-PCR analysis of 12 pairs of fresh clinical tissue samples (Fig. 1C). Similarly, Western blotting results from 12 pairs of fresh clinical tissue samples revealed a significant increase in the expression of SLC35F2 protein in LUAD tissues compared to their paired adjacent normal tissues (Fig. 1 D, E). IHC staining, conducted on 60 pairs of LUAD tissues and their adjacent normal tissues, demonstrated a diffuse distribution of SLC35F2 protein as brown granules in LUAD tissues, while showing minimal staining in the paired adjacent normal tissues (Fig. 2 A-H). In summary, SLC35F2 exhibited a significant upregulation in LUAD tissues when compared to normal tissues.

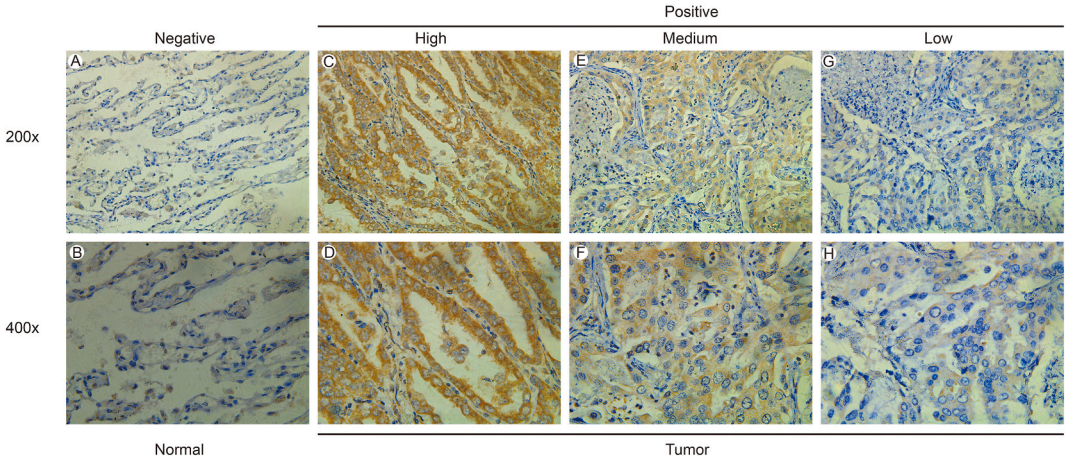


**Fig. 2.** SLC35F2 protein expression in LUAD tissues and adjacent normal tissues. IHC staining showed low SLC35F2 expression (A and B) in paired paracancerous tissues, while LUAD tissues displayed varying degrees of high (C and D), medium (E and F), and low (G and H) expression levels.

### 3.2. The association between SLC35F2 expression and clinicopathological parameters in patients with clinical LUAD

The correlation between SLC35F2 expression and clinicopathological parameters was assessed using IHC staining in a cohort of 60 clinical LUAD patients. Based on the final IHC staining score, the patients were categorized into two groups: high SLC35F2 expression and low SLC35F2 expression. The results revealed that 38 out of 60 patients (63.3 %) exhibited high SLC35F2 expression, while 22 out of 60 patients (36.7 %) had low SLC35F2 expression. The expression of SLC35F2 was significantly associated with tumor size, lymph node metastasis, and clinical stages of LUAD patients (all $P < 0.05$). However, there was no significant correlation observed between SLC35F2 expression and age, gender, depth of invasion, distant metastasis, and serum CEA and CYFRA21-1 levels ($P > 0.05$) (Table 1).

### 3.3. High SLC35F2 expression indicated poor prognosis in LUAD patients

In TCGA datasets, the follow-up period for all subjects ranged from 1 to 227 months, with a median follow-up time of 18.5 months. The Kaplan-Meier curve demonstrated a significant association between high SLC35F2 expression and poorer OS in LUAD patients ($P = 0.016$) (Fig. 3). To determine the independent prognostic factors, Cox regression analysis was performed. Univariate Cox regression analysis revealed that worse OS was correlated with clinical stage (HR: 1.65, 95 % CI: 1.40–1.95, $P < 0.001$), T classification (HR: 1.63, 95 % CI: 1.32–2.02, $P < 0.001$), N classification (HR: 1.79, 95 % CI: 1.46–2.20, $P < 0.001$) and SLC35F2 expression (HR: 1.02, 95 % CI: 1.00–1.05, $P = 0.042$). However, multivariate analysis confirmed that only the clinical stage (HR: 1.95, 95 % CI: 1.22–3.11, $P = 0.005$) was significantly associated with the low survival rate of LUAD patients. Age, gender, TNM staging, and SLC35F2 expression did not demonstrate statistical significance in relation to the survival of LUAD patients ($P > 0.05$) (Table 2).

In the context of clinical LUAD cases, we investigated to examine the potential of SLC35F2 expression as an indicator for recurrence or metastasis. A cohort of 20 recently diagnosed LUAD patients who underwent subsequent treatment was followed up. The duration of follow-up ranged from 9 to 30 months, with a median follow-up time of 20 months. Among these patients, 6 exhibited recurrence or metastasis, all of whom had previously demonstrated high SLC35F2 expression (IHC score 8–12). Notably, during the subsequent follow-up monitoring, 5 out of 6 recurrent cases (83.3 %) displayed elevated CEA levels, while 4 out of 6 recurrent cases (66.7 %) exhibited increased CYFRA21-1 levels. Conversely, no signs of recurrence were observed in the remaining 14 cases, which consistently correlated with the previously observed low or moderate expression of SLC35F2 (IHC score 3–8) (Table 3).

### 3.4. GSEA identified signaling pathways associated with SLC35F2

To ascertain the potential signal pathway associated with the regulated mechanism of SLC35F2, we conducted a comparative analysis of high and low SLC35F2 expression in LUAD using the TCGA database and employing GSEA. The findings suggest a significant correlation between SLC35F2 expression and the following signaling pathways: apoptosis (NES: 1.83, NOM *P*-value: 0.006, FDR q-value: 0.119), adhesion (NES: 1.71, NOM *P*-value: 0.034, FDR q-value: 0.148), small cell lung cancer (SCLC) (NES: 1.69, NOM *P*-value: 0.024, FDR q-value: 0.149), and p53 (NES: 1.96, NOM *P*-value: 0.004, FDR q-value: 0.069) (Fig. 4 A-D, Table 4).

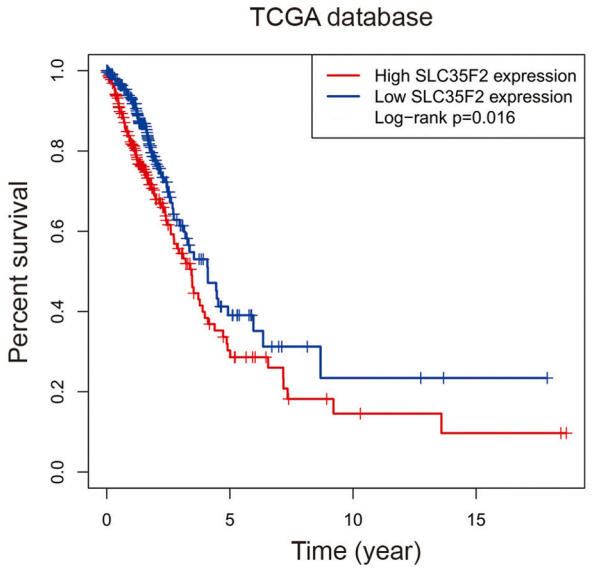


**Fig. 3.** The overall survival of the groups exhibiting high and low expression levels of SLC35F2 in the TCGA datasets.

**Table 2**
Univariate and multivariate Cox regression analysis of various prognostic parameters in TCGA datasets.

| Variables | Univariate analysis | | | Multivariate analysis | | |
|---|---|---|---|---|---|---|
| | HR | 95 % CI | *P* value | HR | 95 % CI | *P* value |
| Age | 1.00 | 0.98–1.02 | 0.843 | 1.01 | 0.99–1.03 | 0.376 |
| Gender | 1.04 | 0.72–1.49 | 0.852 | 0.93 | 0.64–1.36 | 0.708 |
| Stage | 1.65 | 1.40–1.95 | **< 0.001** | 1.95 | 1.22–3.11 | **0.005** |
| T classification | 1.63 | 1.32–2.02 | **< 0.001** | 1.16 | 0.91–1.48 | 0.218 |
| M classification | 1.76 | 0.96–3.20 | 0.066 | 0.39 | 0.12–1.29 | 0.123 |
| N classification | 1.79 | 1.46–2.20 | **< 0.001** | 1.01 | 0.68–1.50 | 0.972 |
| SLC35F2 expression | 1.02 | 1.00–1.05 | **0.042** | 1.02 | 0.99–1.05 | 0.137 |

Abbreviations: HR, hazard ratio; CI, confidence interval.

**Table 3**
Follow-up information of some recently diagnosed and received initial treatment clinical cases.

| No. | Gender | Age | TNM staging | Treatment | Period[#] | SLC35F2 expression | CEA | Cyfra21-1 | Recurrence status |
|---|---|---|---|---|---|---|---|---|---|
| | | (years) | | | (months) | (IHC score) | (ng/mL) | (ng/mL) | |
| 1 | Female | 73 | T2bN0M0, IIA | S | 30 | 4 | 4.4 | 2.36 | NER |
| 2 | Male | 72 | T2bN0M0, IIA | S | 30 | 6 | 1.4 | 1.46 | NER |
| 3 | Female | 30 | T1cN2M0, IIIA | S + C | 20 | 6 | **5.91** | 3.13 | NER |
| 4 | Male | 61 | T2N2M0, IIIA | S + C + R | 15 | 12 | **13.4** | **8.37** | Recurrent LUAD |
| 5 | Female | 64 | T1bN2M0, IIIA | S + C | 18 | 9 | **14.2** | 3.13 | Pleural metastasis |
| 6 | Male | 63 | T2aN1M0, IIB | S + C | 28 | 6 | 2.0 | 1.27 | NER |
| 7 | Male | 53 | T1cN0M0, IA3 | S | 27 | 8 | 3.4 | 1.38 | NER |
| 8 | Male | 70 | T2bN1M0, IIB | S + C | 26 | 8 | **6.5** | 2.20 | NER |
| 9 | Male | 55 | T1bN2M0, IIIA | S + C | 19 | 6 | 2.8 | **5.40** | NER |
| 10 | Female | 42 | T2N2M0, IIIA | S + C + R | 9 | 8 | **8.0** | 3.07 | Bone metastasis |
| 11 | Female | 53 | T2bN0M0, IIA | S | 26 | 6 | 1.8 | 1.26 | NER |
| 12 | Female | 69 | T2aN0M0, IB | S + C | 26 | 3 | 1.5 | 2.64 | NER |
| 13 | Female | 54 | T1bN2M0, IIIA | S + C | 15 | 9 | 1.8 | **4.12** | Recurrent LUAD |
| 14 | Male | 65 | T1bN0M0, IA2 | S | 25 | 8 | **7.2** | 2.76 | NER |
| 15 | Female | 54 | T3N2M0, IIIB | S + C + R | 18 | 12 | **12.4** | **17.23** | Brain metastasis |
| 16 | Female | 49 | T1cN2M0, IIIA | S + C | 22 | 3 | 3.5 | 2.85 | NER |
| 17 | Female | 54 | T2aN1M0, IIB | S + C | 19 | 6 | 2.3 | 2.78 | NER |
| 18 | Female | 66 | T2N1M0, IIB | S + C | 20 | 8 | 2.3 | 3.05 | NER |
| 19 | Female | 43 | T1bN1M0, IIB | S + C | 18 | 8 | 4.3 | 2.56 | NER |
| 20 | Male | 61 | T1cN2M0, IIIA | S + C | 17 | 12 | **10.0** | **5.04** | Contralateral supraclavicular lymph node metastasis |

Abbreviations: S: curatively intended surgery; C: chemotherapy; R: radiation therapy; NER: no evidence of recurrence.
Notes: Boldface in CEA and Cyfra21-1 column represents positive; #: period after treatment; Immunohistochemical (IHC) staining score of $\leq$3 was defined as low SLC35F2 expression and an IHC score of 4–12 was defined as high SLC35F2 expression.

## 4. Discussion

LUAD is a profoundly heterogeneous disease, with the majority of patients receiving a diagnosis in the advanced stages, leading to dismal 5-year survival rates. Clinically, the etiology of LUAD is intricate and diverse, potentially involving numerous genes and pathways. Hence, the identification of novel biomarkers possessing clinicopathological significance and predictive capabilities could enhance the clinical outcomes for LUAD patients. SLC35F2, situated on chromosome 11q22.3, belongs to the human solute carrier family. Additionally, SLC35 encodes nucleotide sugar transporters (NSTs), hydrophobic proteins composed of 320–400 amino acid

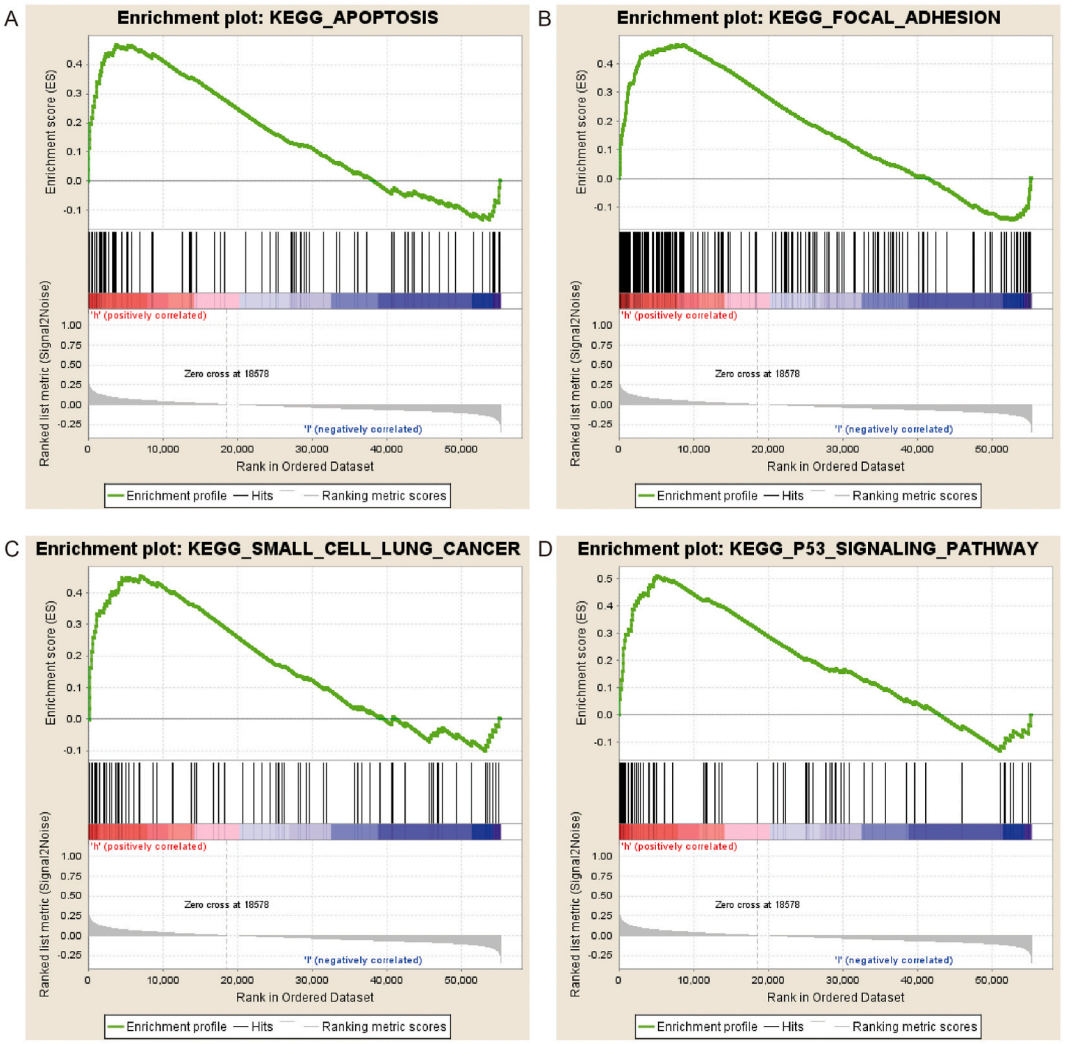


**Fig. 4.** Enrichment plots from GSEA. The GSEA results showcased a significant enrichment of genes associated with SLC35F2 in crucial signaling pathways, including apoptosis signaling (A), adhesion signaling (B), small cell lung cancer signaling (C), and p53 signaling (D) within LUAD cases derived from the TCGA datasets.

**Table 4**
Enrichment parameters of SLC35F2 analyzed by GSEA.

| Gene set name | ES | NES | NOM *P*-value | FDR q-value |
|---|---|---|---|---|
| KEGG_APOPTOSIS | 0.469 | 1.83 | 0.006 | 0.119 |
| KEGG_FOCAL_ADHESION | 0.467 | 1.71 | 0.034 | 0.148 |
| KEGG_SMALL_CELL_LUNG_CANCER | 0.456 | 1.69 | 0.024 | 0.149 |
| KEGG_P53_SIGNALING_PATHWAY | 0.512 | 1.96 | 0.004 | 0.069 |

Abbreviations: ES, enrichment score; NES, normalized enrichment score; NOM, nominal; FDR, false discovery rate.
Notes: Gene sets with NOM *P*-value <0.05 and FDR q-value <0.25 were considered as.
significantly enriched.

residues. SLC35A-E proteins reside in the endoplasmic reticulum and Golgi apparatus, consisting of approximately 10 transmembrane helices. They primarily facilitate the transportation of nucleotide sugars to the Golgi apparatus or the inner lumen of the endoplasmic reticulum, participating in the synthesis of most sugar conjugates [23]. This subtype of NST has been associated with tumor metastasis, cellular immunity, organ development, and morphological characteristics [24]. The SLC35F gene family encompasses five members (F1–F5), and their precise functions remain largely unexplored. Matsuyama et al. demonstrated differential expression of SLC35F in 5-fluorouracil-sensitive tumors compared to drug-resistant tumors [25]. Intriguingly, SLC35F2 is located adjacent to RAB39 on the genome, a significant member of the Ras oncogene family. Moreover, RAB39 has previously been linked to lung cancer, esophageal

cancer, bladder cancer, gastric cancer, and other malignancies [12,13]. Therefore, we hypothesize that SLC35F may play a pivotal role in the tumorigenesis and progression of lung cancer. Currently, only a limited number of studies have focused on the functional roles of SLC35F2 in LUSC [14]. However, the clinical significance of SLC35F2 in the tumorigenesis and progression of LUAD remains unexplored and warrants detailed investigation.

In this study, utilizing bioinformatics analysis of TCGA datasets, we discovered a significant upregulation of SLC35F2 mRNA expression in LUAD tissue compared to normal tissue ($P < 0.05$). Moreover, both qRT-PCR and western blotting experiments confirmed a considerable elevation in SLC35F2 mRNA and protein expression in clinical LUAD tissues as opposed to paired adjacent normal tissues. Additionally, IHC staining revealed high expression of SLC35F2 in 63.3 % of the analyzed clinical LUAD cases (38/60), with significantly higher levels of SLC35F2 protein observed in cancerous tissues compared to adjacent normal tissues. These findings suggest that SLC35F2 expression may serve as a potentially valuable biomarker for LUAD. Furthermore, we conducted an analysis to explore the relationship between IHC expression levels of SLC35F2 and clinicopathological parameters in LUAD patients. Interestingly, the upregulation of SLC35F2 exhibited a close association with tumor size, lymph node metastasis, and clinical stage of LUAD ($P < 0.05$), indicating that SLC35F2 may serve as a molecular biomarker for a subset of patients with more aggressive disease.

Currently, a combination of surgical intervention, radiotherapy, chemotherapy, and targeted therapy is commonly employed for the treatment of LUAD. However, the occurrence of tumor metastasis and recurrence continues to significantly impact the prognosis of patients. To determine whether SLC35F2 can serve as a reliable prognostic factor for LUAD, we utilized the Kaplan Meier plotter and Cox proportional hazards regression to analyze the relationship between survival and SLC35F2 expression levels in TCGA datasets. The Kaplan-Meier curve demonstrated that high expression of SLC35F2 was associated with poor OS in LUAD patients, indicating that SLC35F2 may hold potential for monitoring prognosis. Univariate and multivariate Cox regression analyses indicated that SLC35F2 expression could be a valuable biomarker for assessing LUAD prognosis. Through clinical case analysis, we observed a consistent correlation between high expression of SLC35F2 (IHC score 8–12) and LUAD recurrence, suggesting that SLC35F2 expression may serve as a reliable indicator in monitoring LUAD recurrence or metastasis. Unfortunately, we were unable to collect long-term OS data in clinical LUAD cases. In the future, we plan to further investigate the predictive ability of SLC35F2 expression in tumor recurrence or metastasis by expanding the sample size and extending the follow-up period. Based on these data analyses, it can be concluded that SLC35F2 expression is a prognostic factor for LUAD patients. To gain deeper insights into the underlying mechanisms of SLC35F2 in LUAD, we conducted GSEA using the TCGA database. In terms of biological pathways, the high-SLC35F2 group exhibited enrichment in apoptosis, adhesion, SCLC, and p53 signaling pathways. These findings suggest that the high expression of SLC35F2 may contribute to LUAD development by regulating cell proliferation, apoptosis, division, and differentiation. NSTs, which belong to the SLC35 family of solute carriers, play crucial roles in the glycosylation pathway within the Golgi apparatus and endoplasmic reticulum lumen, providing essential substrates for glycosyltransferases 2, 3 [26]. Previous studies have demonstrated the impact of NSTs, including SLC35F2, on the progression of various cancers. For example, He et al. [17] revealed that NSTs like SLC35F2 influence the progression of PTC by activating the transforming growth factor-β type I receptor (TGFBR1) or apoptosis signal-regulating kinase 1 (ASK-1) or mitogen-activated protein kinase signaling axis. Cheng et al. [27] demonstrated that NST promotes metastasis in hepatocellular carcinoma (HCC) by regulating cellular glycosylation modification and inducing cell adhesion. Yin et al. [28] suggested that choline-induced NSTs, such as SLC5A7, impede colorectal cancer (CRC) growth by stabilizing the p53 protein. Similarly, Che et al. [29] identified that the SLC35F2-SYVN1-TRIM59 axis regulates ferroptosis in pancreatic cancer cells by suppressing endogenous p53. NSTs have been implicated in the progression of various cancers. However, to the best of our knowledge, there are currently no studies reporting the role of NSTs in SCLC. In summary, these studies provide further validation for our findings. Nevertheless, additional experiments are required to further confirm the potential associations between SLC35F2 and cell apoptosis, adhesion, SCLC, and the p53 signaling pathway.

Our study demonstrates that the elevated expression of SLC35F2 holds significant clinical and pathological implications for the prognosis of patients with LUAD. The heightened expression of SLC35F2 serves as an independent predictor of unfavorable prognosis in LUAD patients. Furthermore, SLC35F2 may contribute to the progression of LUAD through its regulation of cell proliferation, apoptosis, division, and differentiation. The expression pattern of SLC35F2 could potentially aid in patient stratification and offer a viable therapeutic target for LUAD patients. However, the validation of SLC35F2's value in fundamental research is currently lacking, and the precise mechanisms remain unclear. These limitations warrant further investigation in future studies.

## Data availability statement

All data generated or analyzed during this study are included in this main text. Data will be made available on request.

## Ethics approval

The study was approved by the Institutional Review Board of Fujian Medical University Union Hospital (Ethics No.: 2021KY050).

## Funding statement

This work was supported by the Startup Fund for Scientific Research, Fujian Medical University (Grant No. 2019QH1019) and the Fujian Provincial Society of Laboratory Medicine and National (Fujian) Genetic Testing Technology Application Demonstration Center (2023LHYC002).

## CRediT authorship contribution statement

**Qingzhu Zheng:** Writing – original draft, Visualization, Project administration, Methodology, Funding acquisition, Formal analysis, Data curation, Conceptualization. **Mingjie Li:** Methodology, Formal analysis, Data curation. **Yingkun Qiu:** Methodology. **Jiahao Yang:** Methodology. **Yingping Cao:** Writing – review & editing, Supervision, Conceptualization.

## Declaration of competing interest

The authors declare that they have no known competing financial interests or personal relationships that could have appeared to influence the work reported in this paper.

## Appendix A. Supplementary data

Supplementary data to this article can be found online at https://doi.org/10.1016/j.heliyon.2023.e23828.

## References

[1] H. Sung, J. Ferlay, R.L. Siegel, M. Laversanne, I. Soerjomataram, A. Jemal, F. Bray, Global cancer statistics 2020: GLOBOCAN estimates of incidence and mortality worldwide for 36 cancers in 185 countries, CA Cancer J Clin 71 (3) (2021) 209–249, https://doi.org/10.3322/caac.21660.
[2] R.L. Siegel, K.D. Miller, A. Jemal, Cancer statistics, 2019, CA Cancer J Clin 69 (1) (2019) 7–34, https://doi.org/10.3322/caac.21551.
[3] Z. Chen, C.M. Fillmore, P.S. Hammerman, C.F. Kim, K.K. Wong, Non-small-cell lung cancers: a heterogeneous set of diseases, Nat. Rev. Cancer 14 (8) (2014) 535–546, https://doi.org/10.1038/nrc3775.
[4] F.R. Hirsch, G.V. Scagliotti, J.L. Mulshine, R. Kwon, W.J. Curran Jr., Y.L. Wu, L. Paz-Ares, Lung cancer: current therapies and new targeted treatments, Lancet 389 (10066) (2017) 299–311, https://doi.org/10.1016/s0140-6736(16)30958-8.
[5] H. Lemjabbar-Alaoui, O.U. Hassan, Y.W. Yang, P. Buchanan, Lung cancer: biology and treatment options, Biochim. Biophys. Acta 1856 (2) (2015) 189–210, https://doi.org/10.1016/j.bbcan.2015.08.002.
[6] D.R. Aberle, A.M. Adams, C.D. Berg, W.C. Black, J.D. Clapp, R.M. Fagerstrom, I.F. Gareen, C. Gatsonis, P.M. Marcus, J.D. Sicks, Reduced lung-cancer mortality with low-dose computed tomographic screening, N. Engl. J. Med. 365 (5) (2011) 395–409, https://doi.org/10.1056/NEJMoa1102873.
[7] S. Ma, L. Shen, N. Qian, K. Chen, The prognostic values of CA125, CA19.9, NSE, AND SCC for stage I NSCLC are limited, Cancer Biomark 10 (3–4) (2011) 155–162, https://doi.org/10.3233/cbm-2012-0246.
[8] Y. Shieh, M. Bohnenkamp, Low-dose CT scan for lung cancer screening: clinical and coding considerations, Chest 152 (1) (2017) 204–209, https://doi.org/10.1016/j.chest.2017.03.019.
[9] T.N. Zamay, G.S. Zamay, O.S. Kolovskaya, R.A. Zukov, M.M. Petrova, A. Gargaun, M.V. Berezovski, A.S. Kichkailo, Current and prospective protein biomarkers of lung cancer, Cancers 9 (11) (2017), https://doi.org/10.3390/cancers9110155.
[10] T. Stankovic, P.J. Byrd, P.R. Cooper, C.M. McConville, D.J. Munroe, J.H. Riley, G.D. Watts, H. Ambrose, G. McGuire, A.D. Smith, A. Sutcliffe, T. Mills, A. M. Taylor, Construction of a transcription map around the gene for ataxia telangiectasia: identification of at least four novel genes, Genomics 40 (2) (1997) 267–276, https://doi.org/10.1006/geno.1996.4595.
[11] L. He, K. Vasiliou, D.W. Nebert, Analysis and update of the human solute carrier (SLC) gene superfamily, Hum Genomics 3 (2) (2009) 195–206, https://doi.org/10.1186/1479-7364-3-2-195.
[12] T. Bangsow, E. Baumann, C. Bangsow, M.H. Jaeger, B. Pelzer, P. Gruhn, S. Wolf, H. von Melchner, D.B. Stanimirovic, The epithelial membrane protein 1 is a novel tight junction protein of the blood-brain barrier, J Cereb Blood Flow Metab 28 (6) (2008) 1249–1260, https://doi.org/10.1038/jcbfm.2008.19.
[13] M. Nishimura, S. Suzuki, T. Satoh, S. Naito, Tissue-specific mRNA expression profiles of human solute carrier 35 transporters, Drug Metabol. Pharmacokinet. 24 (1) (2009) 91–99, https://doi.org/10.2133/dmpk.24.91.
[14] C. Shen, Z. Hui, D. Wang, G. Jiang, J. Wang, G. Zhang, Molecular cloning, identification and analysis of lung squamous cell carcinoma-related genes, Lung Cancer 38 (3) (2002) 235–241, https://doi.org/10.1016/s0169-5002(02)00300-8.
[15] M.D. Nyquist, A. Corella, J. Burns, I. Coleman, S. Gao, R. Tharakan, L. Riggan, C. Cai, E. Corey, P.S. Nelson, E.A. Mostaghel, Exploiting AR-regulated drug transport to induce sensitivity to the survivin inhibitor YM155, Mol. Cancer Res. 15 (5) (2017) 521–531, https://doi.org/10.1158/1541-7786.Mcr-16-0315-t.
[16] R. Kotolloshi, M. Hölzer, M. Gajda, M.O. Grimm, D. Steinbach, SLC35F2, a transporter sporadically mutated in the untranslated region, promotes growth, migration, and invasion of bladder cancer cells, Cells 10 (1) (2021), https://doi.org/10.3390/cells10010080.
[17] J. He, Y. Jin, M. Zhou, X. Li, W. Chen, Y. Wang, S. Gu, Y. Cao, C. Chu, X. Liu, Q. Zou, Solute carrier family 35 member F2 is indispensable for papillary thyroid carcinoma progression through activation of transforming growth factor-β type I receptor/apoptosis signal-regulating kinase 1/mitogen-activated protein kinase signaling axis, Cancer Sci. 109 (3) (2018) 642–655, https://doi.org/10.1111/cas.13478.
[18] G.E. Winter, B. Radic, C. Mayor-Ruiz, V.A. Blomen, C. Trefzer, R.K. Kandasamy, K.V.M. Huber, M. Gridling, D. Chen, T. Klampfl, R. Kralovics, S. Kubicek, O. Fernandez-Capetillo, T.R. Brummelkamp, G. Superti-Furga, The solute carrier SLC35F2 enables YM155-mediated DNA damage toxicity, Nat. Chem. Biol. 10 (9) (2014) 768–773, https://doi.org/10.1038/nchembio.1590.
[19] A.P. Chandrasekaran, K. Kaushal, C.H. Park, K.S. Kim, S. Ramakrishna, USP32 confers cancer cell resistance to YM155 via promoting ER-associated degradation of solute carrier protein SLC35F2, Theranostics 11 (20) (2021) 9752–9771, https://doi.org/10.7150/thno.63806.
[20] L. Bu, G. Jiang, F. Yang, J. Liu, J. Wang, Highly expressed SLC35F2 in non-small cell lung cancer is associated with pathological staging, Mol. Med. Rep. 4 (6) (2011) 1289–1293, https://doi.org/10.3892/mmr.2011.572.
[21] B. Debrabant, The null hypothesis of GSEA, and a novel statistical model for competitive gene set analysis, Bioinformatics 33 (9) (2017) 1271–1277, https://doi.org/10.1093/bioinformatics/btw803.
[22] A. Subramanian, P. Tamayo, V.K. Mootha, S. Mukherjee, B.L. Ebert, M.A. Gillette, A. Paulovich, S.L. Pomeroy, T.R. Golub, E.S. Lander, J.P. Mesirov, Gene set enrichment analysis: a knowledge-based approach for interpreting genome-wide expression profiles, Proc Natl Acad Sci U S A 102 (43) (2005) 15545–15550, https://doi.org/10.1073/pnas.0506580102.
[23] N. Ishida, M. Kawakita, Molecular physiology and pathology of the nucleotide sugar transporter family (SLC35), Pflugers Arch 447 (5) (2004) 768–775, https://doi.org/10.1007/s00424-003-1093-0.
[24] B. Hadley, A. Maggioni, A. Ashikov, C.J. Day, T. Haselhorst, J. Tiralongo, Structure and function of nucleotide sugar transporters: current progress, Comput. Struct. Biotechnol. J. 10 (16) (2014) 23–32, https://doi.org/10.1016/j.csbj.2014.05.003.
[25] R. Matsuyama, S. Togo, D. Shimizu, N. Momiyama, T. Ishikawa, Y. Ichikawa, I. Endo, C. Kunisaki, H. Suzuki, Y. Hayasizaki, H. Shimada, Predicting 5-fluorouracil chemosensitivity of liver metastases from colorectal cancer using primary tumor specimens: three-gene expression model predicts clinical response, Int. J. Cancer 119 (2) (2006) 406–413, https://doi.org/10.1002/ijc.21843.

[26] J.L. Parker, S. Newstead, Structural basis of nucleotide sugar transport across the Golgi membrane, Nature 551 (7681) (2017) 521–524, https://doi.org/10.1038/nature24464.
[27] H. Cheng, S. Wang, D. Gao, K. Yu, H. Chen, Y. Huang, M. Li, J. Zhang, K. Guo, Nucleotide sugar transporter SLC35A2 is involved in promoting hepatocellular carcinoma metastasis by regulating cellular glycosylation, Cell. Oncol. 46 (2) (2023) 283–297, https://doi.org/10.1007/s13402-022-00749-7.
[28] Y. Yin, Z. Jiang, J. Fu, Y. Li, C. Fang, X. Yin, Y. Chen, N. Chen, J. Li, Y. Ji, X. Su, M. Qiu, W. Huang, B. Zhang, H. Deng, L. Dai, Choline-induced SLC5A7 impairs colorectal cancer growth by stabilizing p53 protein, Cancer Lett. 525 (2022) 55–66, https://doi.org/10.1016/j.canlet.2021.09.027.
[29] B. Che, Y. Du, R. Yuan, H. Xiao, W. Zhang, J. Shao, H. Lu, Y. Yu, M. Xiang, L. Hao, S. Zhang, X. Du, X. Liu, W. Zhou, K. Wang, L. Chen, SLC35F2-SYVN1-TRIM59 axis critically regulates ferroptosis of pancreatic cancer cells by inhibiting endogenous p53, Oncogene (2023), https://doi.org/10.1038/s41388-023-02843-y.